One-pot synthesis of spring-like superstructures consisting of layered tin(IV) hydrogen phosphate nanodisks†

Hui Qiao,[a] Falong Jia,[a] Zhihui Ai,[a] Zhaosheng Li[b] and Lizhi Zhang*[a]

Received (in Cambridge, UK) 23rd January 2006, Accepted 21st March 2006
First published as an Advance Article on the web 6th April 2006
DOI: 10.1039/b601057a

Spring-like superstructures consisting of layered tin(IV) hydrogen phosphate nanodisks can be obtained *via* a one-pot solvothermal reaction of tin tetrachloride and phosphoric acid in ethanol. These superstructures are active anode materials for the lithium-ion battery.

The synthesis of organized extended structures based on the assembly of nanostructured building blocks has attracted much attention because the resulting hierarchical, multi-functional materials can be applied in various fields such as catalysis, medicine, electronics, ceramics, pigments, and cosmetics.[1,2] A number of strategies have been developed to spatially pattern and control higher-order organization. For instance, molecular cross-linking,[3] a DNA-based method,[4] chemical and microfabrication methods,[5] and self-assembly formation of superlattices,[6] *etc.* were utilized to different superstructures of metal,[7] and oxide.[5] In recent years, a variety of superstructures of sulfates, chromates, tungstates, molybdates, silicates, and carbonates have been synthesized in reverse micelles.[8] Alternatively, bioinspired morphosynthesis strategies have also been explored to template inorganic superstructures, by using self-assembled organic superstructures, organic additives, and/or templates with complex functionalization patterns.[9]

The phosphates of tetravalent metals possess attractive physical and chemical properties. These metallic phosphates have the general formula $M(HPO_4)_2{\cdot}H_2O$, where M stands for a tetravalent cation (*e.g.* Zr, Ti, Hf, Ge, Sn, Pb). The crystalline form of these solids exhibits a planar layered structure, which is made up of $[M(PO_4)_2]_n^{2n-}$ macroanions.[10] An equivalent number of protons forming weak PO–H bonds compensate the negative charge of the oxygen atoms. These acid protons can be easily replaced by other cation species without producing any structural change of the layered host lattice. Great interest has been directed toward the search for new layered phosphates of tetravalent metals since the 1960s due to their potential applications as ion exchangers, proton conductors, sensors, and catalysts for heterogeneous acid-catalyzed reactions.[11,12]

In this communication, we demonstrate that a novel complex architectures of layered tin(IV) hydrogen phosphate (α-SnP) can be obtained *via* a one-pot solvothermal reaction of tin tetrachloride and phosphoric acid in ethanol. Uniform nanodisks of α-SnP connect into spring-like superstructures without any organic surfactants or biomolecules. To the best of our knowledge, this is the first example to report such superstructures of α-SnP.

In a typical procedure, 0.35 g of $SnCl_4{\cdot}5H_2O$ (AR) was added to 12 mL of anhydrous ethanol. Then 0.3 mL of H_3PO_4 (85%) was added to the above solution. The resulting solution was transferred to a 22 ml Teflon-sealed autoclave and stored at 180 °C for 24 h, then air-cooled to room temperature. The products were washed several times with anhydrous ethanol, and finally dried at 60 °C in a vacuum-oven.

X-ray diffraction (XRD) patterns of the products were recorded on a Rigaku D/MAX-RB diffractometer with monochromatized Cu Kα radiation (λ = 1.5418 Å). Fig. 1 shows the XRD pattern of the as-synthesized product. All the diffraction peaks can be well indexed to those of $Sn(HPO_4)_2{\cdot}H_2O$ (JCPDS, no. 31-1397). The lattice constants can be calculated as follows: a = 8.618(5) Å, b = 4.974(3) Å, c = 15.616(5) Å, and β = 100.42°, which are consistent with the literature values.

The morphologies of the products were investigated by a scanning electron microscope (SEM, JSM-5600). Fig. 2 shows the SEM images of nanostructures of $Sn(HPO_4)_2{\cdot}H_2O$. It is found that there are plenty of spring-like superstructures in the product (Fig. 2a). These superstructures are a little similar to stacked

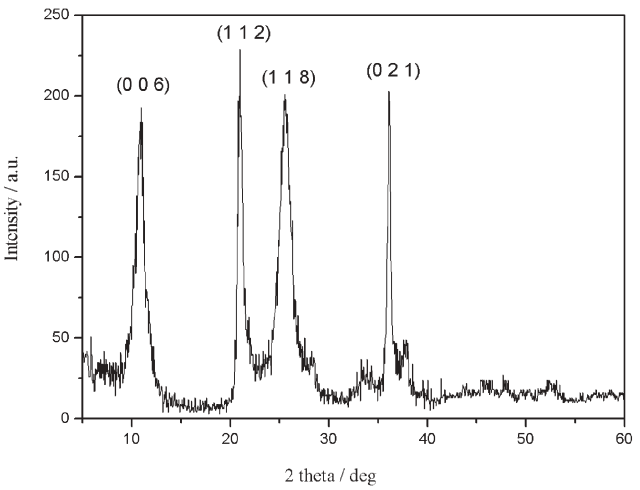

Fig. 1 XRD patterns of the resulting sample obtained in the presence of 0.3 mL of H_3PO_4 at 180 °C for 24 h.

[a]*Key Laboratory of Pesticide and Chemical Biology, Ministry of Education, College of Chemistry, Central China Normal University, Wuhan, Hubei, 430079, P. R. China. E-mail: zhanglz@mail.ccnu.edu.cn; Fax: 86 276786 7535; Tel: 86 276786 7535*
[b]*Ecomaterials and Renewable Energy Research Center, Department of Physics, Nanjing University, Jiangsu, 210093, P. R. China*

† Electronic supplementary information (ESI) available: XRD patterns, SEM images of $Sn(HPO_4)_2{\cdot}H_2O$ prepared under different conditions. Crystal structure of $Sn(HPO_4)_2{\cdot}H_2O$. FTIR spectrum, TGA-DTA curves and charge–discharge properties of $Sn(HPO_4)_2{\cdot}H_2O$ superstructures. See DOI: 10.1039/b601057a

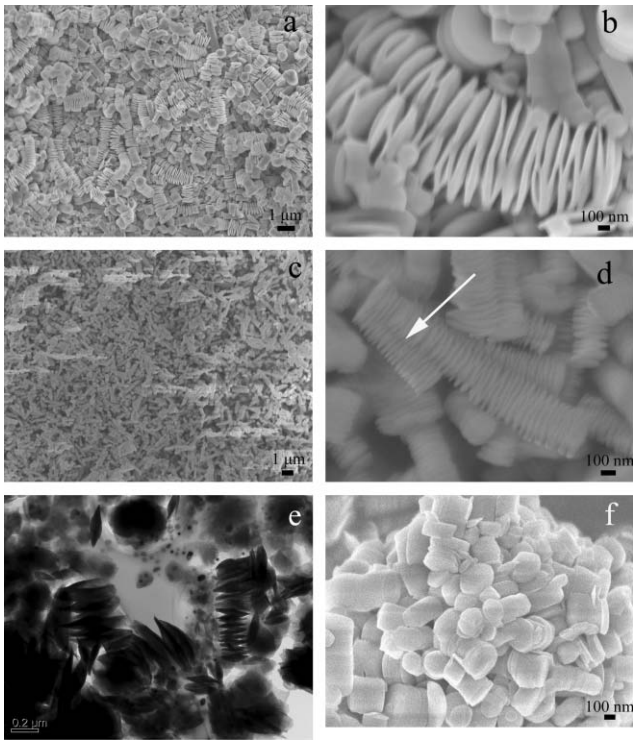

Fig. 2 (a, b) SEM images of the resulting $Sn(HPO_4)_2{\cdot}H_2O$ superstructures obtained in the presence of 0.3 mL H_3PO_4 *via* solvothermal reaction for 24 h. (c, d) SEM images of the resulting $Sn(HPO_4)_2{\cdot}H_2O$ superstructures obtained in the presence of 0.3 mL H_3PO_4 *via* solvothermal reaction for 48 h. (e) TEM image of the resulting $Sn(HPO_4)_2{\cdot}H_2O$ superstructures obtained in the presence of 0.3 mL H_3PO_4 *via* solvothermal reaction for 24 h. (f) SEM image of the $Sn(HPO_4)_2{\cdot}H_2O$ rod obtained in the presence of 0.3 mL H_3PO_4 *via* solvothermal reaction for 6 h.

calcium carbonate (calcite) superstructures consisting of pseudo-hexagonal plates, which were prepared by a microemulsion-based method.[1] Here the superstructures are 0.5 to 5 micrometer in length. Each superstructure consists of many nanodisks of about 400 to 800 nm in diameter. A higher magnification SEM image (Fig. 2b) shows that the middle of a single disk is thicker than the edge. The edges are about 20 nm in thickness. All the neighbouring disks connect with each other at the middle. Meanwhile, some of neighbouring disks also connect at the edge. This gives the nanostructures the appearance of springs.

We examined the factors affecting the formation of the spring-like superstructures of $Sn(HPO_4)_2{\cdot}H_2O$. It was found that the amount of H_3PO_4 in the solution can affect the diameters of nanodisks. For example, when the amount of H_3PO_4 was increased from 0.3 mL to 0.6 mL, the diameters of the nanodisks in the superstructures were in the range of 300 to 500 nm (Supplementary Information†). When the reaction time was increased from 24 h to 48 h without changing the amount of H_3PO_4, the spring-like superstructures became more uniform. All the superstructures were 2 to 4 micrometer in length (Fig. 2c). Moreover, the nanodisks in the superstructures became thinner and smaller (Fig. 2d). Interestingly, some superstructures crossed over each other (indicated by an arrow in Fig. 2d). However, when de-ionized water was used instead of anhydrous ethanol, no solid sample could be obtained. If there was too much water in the reaction system, $Sn(HPO_4)_2{\cdot}H_2O$ spring-like superstructures could not form. So it could be concluded that excess water inhibits the formation of $Sn(HPO_4)_2{\cdot}H_2O$ spring-like superstructures (Supplementary information†).

The structure and morphology of the product were further characterized by transmission electron microscopy (TEM, Philip CM 120). The TEM image (Fig. 2e) confirms the spring-like superstructure of the product with the middle of each disk thicker than the edge. The nanosprings are "robust" enough to tolerate the sonication conditions in the preparation of sample for TEM measurements without being destroyed. Unfortunately, we could not obtain the selected area diffraction pattern and high resolution TEM of the nanodisks because of their instability under electron beams.

The infrared spectra of nanostructure $Sn(HPO_4)_2{\cdot}H_2O$ was recorded on a Fourier infrared spectrum instrument (Nicolet Magna-IR 750, Supplementary information†). Wide bands at 3000 cm^{-1} are typical of the stretching vibration mode of the OH of water embedded in the structure. The breadth of this peak is due to hydrogen bonding.[13,14] The bands appearing in the 900–1200 cm^{-1} spectral region are assigned to symmetric and antisymmetric stretching of P–O bonds pertaining to PO_4 groups.[15] The band at 1631 cm^{-1} is due to the OH vibration of water molecules coordinated to the phosphate groups. The existence of several bands in the 400–700 cm^{-1} region as well as the presence of two bands at 3360 cm^{-1} and 3485 cm^{-1} are due to P–OH and Sn–OH stretching vibrations and stretching vibrations of OH bonding to P and Sn,[13,16,17] respectively. The 3485 cm^{-1} signal is caused by bond vibrations between the Sn atoms present in the lamellae and the OH groups belonging to the molecules of water of crystallization that are present in the interlamellar region of the structure.[18]

Thermogravimetric analysis (TGA) reveals that the final product decomposes in two steps (Supplementary information†). The first step occurs between 100 and 220 °C. The weight loss in this step is 5.2%, which corresponds to the dehydration of $Sn(HPO_4)_2{\cdot}H_2O$ (calc. 5.5%). This results in the anhydrous acid phosphate $Sn(HPO_4)_2$.[10] In the second step from 220 to 600 °C, a condensation process occurs. One more water molecule is released to form a layered pyrophosphate SnP_2O_7.[10] From 600 °C onwards, a gradual continuous mass loss takes place, due to the final transformation to SnO_2, which was proved by the X-ray diffraction.

Although the formation mechanism of spring-like superstructures is unclear at present, we believe it may be related to the crystal structure of $Sn(HPO_4)_2{\cdot}H_2O$. The structure is built up of layers of slightly distorted SnO_6 octahedral and alternating HPO_4 tetrahedral (Fig. 3). After examining the samples collected at different reaction stages by SEM and XRD, we may speculate the formation process of spring-like superstructures of $Sn(HPO_4)_2{\cdot}H_2O$ as follows. First, $Sn(HPO_4)_2{\cdot}H_2O$ rods form at the early stage of reaction (Fig. 2f). Then, these rods transfer into spring-like superstructures consisting of nanodisks during further crystallization under solvothermal treatment (Fig. 2a).

We also studied the charge–discharge property of $Sn(HPO_4)_2{\cdot}H_2O$ spring-like superstructures as anode materials for the lithium-ion battery. It showed an initial high discharge specific capacity of 373.7 mAh g^{-1} in the potential range of 2.0–0.0 V. This indicates

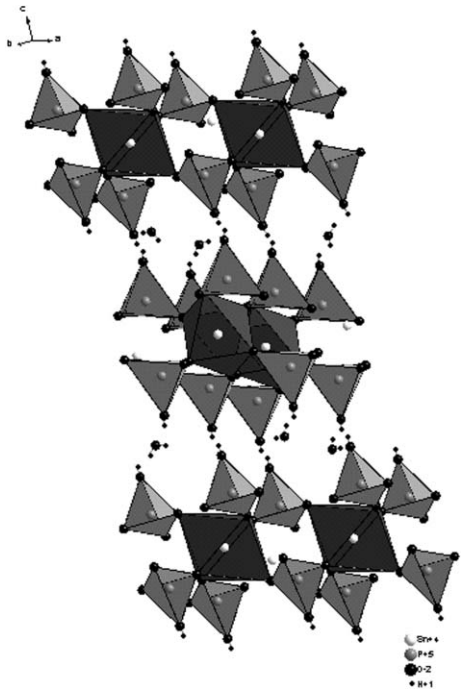

Fig. 3 Crystal structure of $Sn(HPO_4)_2 \cdot H_2O$.

that the $Sn(HPO_4)_2 \cdot H_2O$ spring-like superstructures may be promising anode materials for the lithium-ion battery. Detailed studies on the formation mechanism and electrochemical properties of these spring-like superstructures are in progress.

The work described in this paper was partially supported by National Science Foundation of China (20503009) and Open Fund of Hubei Key Laboratory of Catalysis and Materials Science (CHCL0508).

Notes and references

1 C. Viravaidya, M. Li and S. Mann, *Chem. Commun.*, 2004, 2182.
2 S. H. Yu, H. Cölfen and M. Antonietti, *Chem.–Eur. J.*, 2002, **13**, 2937.
3 M. Brust, D. Bethell, D. J. Schiffrinand and C. J. Kiely, *Adv. Mater.*, 1995, **7**, 795.
4 C. A. Mirkin, R. L. Letsinger, R. C. Mucic and J. J. Storhoff, *Nature*, 1996, **382**, 607.
5 P. D. Yang, A. H. Rizvi, B. Messer, B. F. Chmelka, G. M. Whitesides and G. D. Stucky, *Adv. Mater.*, 2001, **13**, 427.
6 Z. L. Wang, *Adv. Mater.*, 1998, **10**, 13.
7 K. V. Sarathy, G. U. Kulkarni and C. N. R. Rao, *Chem. Commun.*, 1997, 537.
8 H. T. Shi, L. M. Qi. J. M. Ma and N. Z. Wu, *Adv. Funct. Mater.*, 2005, **15**, 442; H. T. Shi, L. M. Qi. J. M. Ma, H. M. Cheng and B. Y. Zhu, *Adv. Mater.*, 2005, **15**, 1647; S. H. Yu, H. Cölfen and M. Antonietti, *J. Phys. Chem. B*, 2003, **107**, 7396; H. Cölfen and M. Antonietti, *Angew. Chem., Int. Ed.*, 2005, **44**, 5576.
9 M. Antonietti, M. Breulmann, C. G. Goltner, H. Cölfen, K. K. W. Wong, D. Walsh and S. Mann, *Chem.–Eur. J.*, 1998, **4**, 2493; N. Nassif, N. Gehrke, N. Pinna, N. Shirshova, K. Tauer, M. Antonietti and H. Cölfen, *Angew. Chem., Int. Ed.*, 2005, **44**, 6004; N. Gehrke, H. Cölfen, N. Pinna, M. Antonietti and N. Nassif, *Cryst. Growth Des.*, 2005, **5**, 1317; A. W. Xu, Q. Yu, W. F. Dong, M. Antonietti and H. Cölfen, *Adv. Mater.*, 2005, **17**, 2217; K. Aoki and S. Mann, *J. Mater. Chem.*, 2005, **15**, 113.
10 C. Veläsquez, F. Rojas, V. H. Lara and A. Campero, *Phys. Chem. Chem. Phys.*, 2004, **6**, 4714; S. Bruque, M. A. G. Aranda, E. R. Losilla, P. Olivera-Pastor and P. Maireles-Torres, *Inorg. Chem.*, 1995, **34**, 893; J. X. Chen, M. G. Liu, H. J. Pan, S. F. Lin and X. Q. Xin, *J. Solid State Chem.*, 2001, **159**, 130.
11 J. M. Tarascon and M. Armand, *Nature*, 2001, **414**, 359.
12 P. G. Bruce, *Chem. Commun.*, 1997, 1817.
13 G. Busca, G. Ramis, V. Lorenzelli, P. F. Ross, A. L. Ginestra and P. Patrono, *Langmuir*, 1989, **5**, 911.
14 J. M. Lewis and R. A. Kydd, *J. Catal.*, 1991, **132**, 465.
15 A. Rulmont, R. Cahay, M. L. Duyckaerts and P. Tarte, *Eur. J. Solid State Inorg. Chem.*, 1991, **28**, 207.
16 B. Rebenstor, T. Linhlad and S. L. T. Anderson, *J. Catal.*, 1991, **128**, 293.
17 J. B. Peri, *Discuss. Faraday Soc.*, 1971, **52**, 55.
18 B. B. Sahu, H. K. Mishra and K. Parida, *J. Colloid Interface Sci.*, 2000, **225**, 511.